The impact of a shock-wave on a thin two-dimensional aerofoil moving at supersonic speed

By J. L. SMYRL

Department of Mathematics, Royal College of Science and Technology, Glasgow

(Received 15 May 1961 and in revised form 8 October 1962)

The pressure field is found in closed analytic form for the region behind an arbitrary plane shock, which has encountered a thin aerofoil moving at supersonic speed. The solution may be used for wedges at small incidence to the air-flow around them, and for wedges yawed with respect to the shock plane through angles up to a limiting value which always exceeds 67·8°. The pressure distribution on the surface of a wedge is calculated in a number of examples illustrating separately the effects of shock strength, wedge speed, and angle of yaw.

1. Introduction

The flow resulting when a plane shock-wave meets normally a thin infinite wedge at rest relative to the surrounding air was found by Lighthill (1949). A solution applicable not only to wedges but to any thin symmetric aerofoil was given by Ludloff & Ting (1951, 1952). Chester (1954) extended the work of Lighthill to include infinite wedges at yaw. The present paper is concerned with a plane shock-wave meeting a thin aerofoil which is moving in the opposite direction at supersonic speed; small angles of incidence are permitted and the aerofoil may be yawed up to a certain limit. The problem is of practical interest in connexion with blast effects on supersonic aircraft.

Ehlers & Shoemaker (1959) have solved the problem of a weak shock-wave meeting, at any angle of incidence, a flat plate moving subsonically or supersonically. In contrast, the present problem concerns a shock-wave of arbitrary strength, and the supersonic aerofoil has a weak attached shock so that a collision between two shocks is involved.

The solution is given first for a thin infinite wedge; the problem is linearized and the methods of solution based on those of Lighthill and Chester. New features include a contact discontinuity resulting from the shock collision, and it is shown that the boundary-value problem for pressure is unaffected by the presence of this discontinuity in the other variables. The pressure is expressed in terms of elementary functions, and in particular expressions are found for the pressure on the surface of the wedge, and along the shock, in terms of the basic co-ordinates. Numerical examples are given for various shock strengths, wedge speeds, and angles of yaw. Finally, the solutions are extended to cover the case of a thin aerofoil of arbitrary shape.

2. Wedge and normal shock

We consider first a plane shock, the plane of which coincides at time $t = 0$ with the (Y, Z)-plane, moving with velocity U in the direction of the X-axis into a uniform region (0) of still air. A thin wedge of infinite span, whose leading edge coincides at time $t = 0$ with the Z-axis and whose plane of symmetry lies approximately in the (X, Z)-plane, moves with supersonic velocity W in the direction of the negative X-axis. When $t \leqslant 0$ the flow pattern consists of three uniform regions (0), (1), (2); regions (0) and (1) are separated by the shock, while regions (0) and (2) are separated by weak bow shock-waves attached to the leading edge. We seek a solution to the flow problem for $t > 0$ and we note the following simplifying features: (i) the flow is independent of Z; (ii) since the flow is at all times supersonic relative to the wedge, the flow patterns on the two sides of the wedge are independent; it is therefore sufficient to find the solution for $Y > 0$; (iii) there is no fundamental length in the data defining the problem. We denote by p, ρ, $\mathbf{V}$ and c the respective flow variables pressure, density, flow velocity and sound speed; by virtue of (i) and (iii) these are functions of X/t, Y/t only. The conservation relations across a stationary shock may be written in the form

$$\left.\begin{aligned} \mathbf{V}_b &= \mathbf{V}_a + \tfrac{5}{6}(\mathbf{V}_a\cdot\mathbf{n})\,[\{c_a^2/(\mathbf{V}_a\cdot\mathbf{n})^2\} - 1]\,\mathbf{n}, \\ p_b &= \tfrac{5}{6}\rho_a[(\mathbf{V}_a\cdot\mathbf{n})^2 - \tfrac{1}{7}c_a^2], \\ \rho_b &= 6\rho_a/[1 + 5c_a^2/(\mathbf{V}_a\cdot\mathbf{n})^2], \end{aligned}\right\} \qquad (2.1)$$

where $\mathbf{n}$ is the unit normal to the shock front, suffices a, b refer to values ahead of and behind the shock, respectively, and the adiabatic index of air is taken to be 1·4.

Numerical suffices are used with any variable to denote its constant value in the uniform region of the same number. Thus if ϵ (supposed small) is the angle between the wedge face and the (X, Z)-plane, we have (Courant & Friedrichs 1948)

$$p_2 = p_0 + \epsilon\rho_0 W^2 \tan\phi_0, \quad \rho_2 = \rho_0[1 + \epsilon(W/c_0)^2 \tan\phi_0], \quad \mathbf{V}_2 = \{-\epsilon W \tan\phi_0, \epsilon W\},$$

$$c_2 = c_0[1 + \epsilon(W^2/5c_0^2)\tan\phi_0], \quad \phi_0 = \sin^{-1}(c_0/W).$$

The Mach number $M(= U/c_0)$ of the shock and the Mach number $M'(= W/c_0)$ of the wedge are the fundamental data defining the problem. Writing $M_1(= V_1/c_1)$ for the Mach number of the uniform flow behind the shock, we find from equations (2.1) that

$$M_1 = 5(M^2 - 1)/[(7M^2 - 1)(M^2 + 5)]^{\frac{1}{2}}, \quad c_1/c_0 = [(7M^2 - 1)(M^2 + 5)]^{\frac{1}{2}}/6M.$$

The main flow regions for $t > 0$ are indicated in figure 1. The leading edge is represented by the point L, I is the intersection of the shock and the bow-wave, and the axes are moving with the velocity $\mathbf{V}_1$ of the flow in region (1). The presence of the wedge in region (1) causes a small disturbance; the limit of the spread of this disturbance is a circle, centre O, radius $c_1 t$, together with the tangent LC and the shock front. Furthermore, some alteration in the position of the intersecting shocks below I is necessary (see von Mises 1958) and we are led to make the following assumptions.

(i) The shock is deflected at I through a small angle δ (say) which we measure positive when anti-clockwise.

(ii) The bow-wave is deflected at I into the position of the tangent ID, and a new bow-wave is formed in the position of the tangent LC.

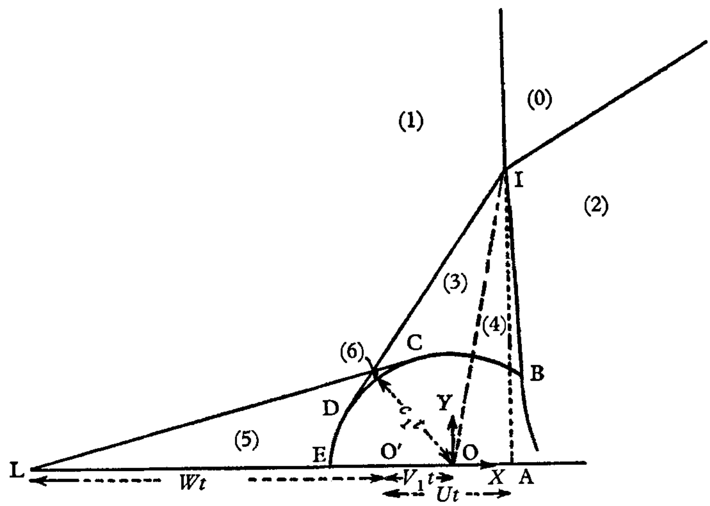

FIGURE 1. The main flow regions after the wedge has penetrated the shock front.

(iii) A contact discontinuity, in the approximate position IO, divides the air behind the shock front into two non-mixing portions, that which crossed the shock front directly from region (0) being thus separated from that which first crossed the bow-wave into region (2).

(iv) Outside the sonic circle the flow consists only of uniform regions. In particular, the shock front is straight except for the portion AB which must bend so as to meet the wedge face normally.

These assumptions provide the smallest and simplest disturbed region consistent with the physical facts and for which a solution can be found. Figure 2, plate 1, shows the analogous situation in shallow-water theory and supports many of the above hypotheses.

All regions of uniform flow are denoted by numbers (see figure 1). Region (6) exists only when the tangents LC, ID intersect and is then a straightforward superposition of the disturbances in regions (3) and (5) since the intersecting shocks are both weak (see von Mises 1958). In terms of the shock strength λ, where

$$\lambda = \rho_1/\rho_0 = 6M^2/(M^2+5),$$

it is found that LC and ID intersect unless

$$M' > \sqrt{5}\,(\lambda-1)/\{(6\lambda-1)^{\frac{1}{2}} - \lambda^{\frac{1}{2}}(6-\lambda)^{\frac{1}{2}}\},$$

but the solution procedure is unaffected. (Non-intersecting tangents in the first-order theory correspond, in the physical problem, to the bow-wave becoming *concave* towards the wedge.) The tangent ID vanishes completely if the point I falls within the sonic circle. This cannot happen for shock strengths up to $\lambda = \sqrt{6}$, and thereafter only if

$$M' > [\lambda\{5\lambda(6-\lambda)\}^{\frac{1}{2}} + 6(\lambda-1)(\lambda+1)^{\frac{1}{2}}]/(\lambda^2-6).$$

Some adjustment to the solution procedure is necessary in this case (see § 8). Since $1 < \lambda < 6$ for all real shocks, figure 3 illustrates the range of M' and λ corresponding to the three cases.

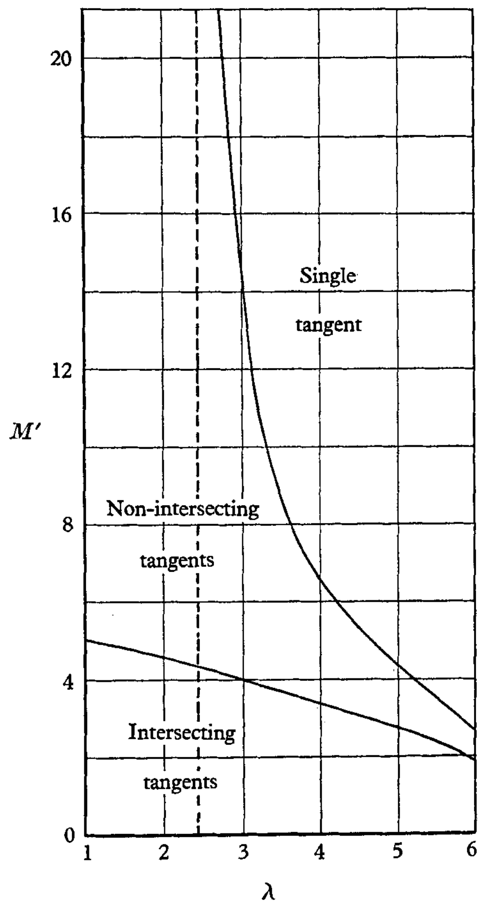

FIGURE 3. The dependence on M' and λ of the proposed flow picture in figure 1.

3. The non-uniform region

Since air enters this region across a curved shock we expect rotational motion. The equations of two-dimensional unsteady rotational motion are

$$\left.\begin{aligned} \partial\rho/\partial t + \nabla.(\rho\mathbf{V}) &= 0, \\ \partial\mathbf{V}/\partial t + (\mathbf{V}.\nabla)\mathbf{V} &= -(1/\rho)\nabla p, \\ (\partial/\partial t + \mathbf{V}.\nabla)(p\rho^{-1\cdot 4}) &= 0. \end{aligned}\right\} \quad (3.1)$$

For any thin wedge the disturbed flow must be no more than a small perturbation away from the uniform flow of region (1). Consequently, we think of ϵ as a parameter and assume Taylor expansions of the form

$$\left.\begin{aligned} p &= p_1+\epsilon p^{(1)}(X, Y, t)+\epsilon^2 p^{(2)}(X, Y, t)+\ldots, \\ \rho &= \rho_1+\epsilon \rho^{(1)}(X, Y, t)+\epsilon^2 \rho^{(2)}(X, Y, t)+\ldots, \\ \mathbf{V} &= \qquad \epsilon \mathbf{V}^{(1)}(X, Y, t)+\epsilon^2 \mathbf{V}^{(2)}(X, Y, t)+\ldots, \end{aligned}\right\} \tag{3.2}$$

for the disturbed flow. Substituting from equations (3.2) into equations (3.1) and equating coefficients of ϵ now gives

$$\left.\begin{aligned} \partial\rho'/\partial t+c_1\nabla.\mathbf{V}' &= 0, \\ \partial\mathbf{V}'/\partial t+c_1\nabla p' &= 0, \\ \partial p'/\partial t &= \partial\rho'/\partial t, \end{aligned}\right\} \tag{3.3}$$

where the results have been expressed in terms of non-dimensional variables

$$p' = p^{(1)}/\rho_1 c_1^2, \quad \rho' = \rho^{(1)}/\rho_1, \quad \mathbf{V}' = \mathbf{V}^{(1)}/c_1 = \{u', v'\}.$$

The 'cone-field' property of the problem enables us to reduce the number of independent variables to two by setting $x = X/c_1 t$, $y = Y/c_1 t$. Since p', ρ', $\mathbf{V}'$ are functions of x and y only, equations (3.3) may be written as

$$\left.\begin{aligned} x\frac{\partial p'}{\partial x}+y\frac{\partial p'}{\partial y} &= \frac{\partial u'}{\partial x}+\frac{\partial v'}{\partial y}, \\ x\frac{\partial u'}{\partial x}+y\frac{\partial u'}{\partial y} &= \frac{\partial p'}{\partial x}, \\ x\frac{\partial v'}{\partial x}+y\frac{\partial v'}{\partial y} &= \frac{\partial p'}{\partial y}, \\ x\frac{\partial p'}{\partial x}+y\frac{\partial p'}{\partial y} &= x\frac{\partial \rho'}{\partial x}+y\frac{\partial \rho'}{\partial y}. \end{aligned}\right\} \tag{3.4}$$

Elimination of u' and v' from the first three of equations (3.4) gives an equation for p' only, viz.

$$\nabla^2 p' = \left(x\frac{\partial}{\partial x}+y\frac{\partial}{\partial y}+1\right)\left(x\frac{\partial p'}{\partial x}+y\frac{\partial p'}{\partial y}\right). \tag{3.5}$$

In the (x, y)-plane the flow pattern appears 'steady' and figure 4 indicates its main features.

The points $\mathrm{B}(x_0, y_0)$, $\mathrm{C}(x_1, y_1)$, $\mathrm{D}(x_2, y_2)$ and E lie on the circumference of the unit circle, centre O, and the co-ordinates of B, C, D and $\mathrm{I}(x_0, y_3)$ are given by

$$\begin{aligned} x_0 &= (U-V_1)/c_1 = \{(M^2+5)/(7M^2-1)\}^{\frac{1}{2}}, \\ y_3 &= \{(W+U)/c_1\}\tan\phi_0 = [6M(M+M')]/[(7M^2-1)(M^2+5)(M'^2-1)]^{\frac{1}{2}}, \\ x_1 &= -1/(M_1+c_0 M'/c_1), \\ x_2 &= -\{y_3(x_0^2+y_3^2-1)^{\frac{1}{2}}-x_0\}/(x_0^2+y_3^2), \\ y_i &= (1-x_i^2)^{\frac{1}{2}} \quad (i = 0, 1, 2). \end{aligned}$$

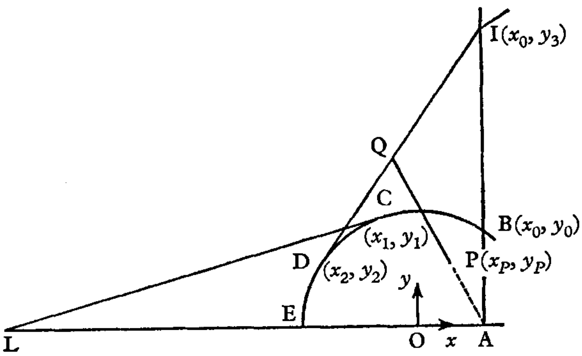

FIGURE 4. The disturbed region in the (x, y)-plane.

4. Boundary conditions for p' in the non-uniform region

On the circular arc BCDE p' takes constant values with discontinuities at C and D. We denote by p'_i the value of p' appropriate to the uniform region (i) and, where required, a similar suffix notation is used with ρ', u', v'. We must have $p'_3 = p'_4$ and (see Courant & Friedrichs 1948)

$$p'_5 = \{(c_0/c_1)\, M' + M_1\}^2/[\{(c_0/c_1)\, M' + M_1\}^2 - 1]^{\frac{1}{2}}.$$

If region (6) exists we have $p'_6 = p'_3 + p'_5$ so that only p'_3 need now be determined.

To establish the conditions at the shock front, we take the position of the shock front to be given by the equation

$$x = x_0 + \epsilon f(y) + O(\epsilon^2),$$

where $f(y)$ is as yet unknown. The shock equations (2.1) now give, after some simplification, that

$$\left.\begin{aligned} u' &= \frac{5}{6}\left\{\left(1+\frac{1}{M^2}\right)\{f(y)-yf'(y)\} + (M'^2-1)^{-\frac{1}{2}}\frac{c_0}{c_1}\left(\frac{M'}{M^2} - \tfrac{1}{5}M' - \frac{2}{5}\frac{M'^2}{M}\right)\right\},\\ v' &= -M_1 f'(y) + (c_0/c_1)\, M',\\ p' &= \frac{5}{3}\frac{\rho_0}{\rho_1}\frac{c_0}{c_1}\left\{M\{f(y)-yf'(y)\} + (M'^2-1)^{-\frac{1}{2}}\frac{c_0}{c_1}(MM' + \tfrac{1}{2}M^2M'^2 - \tfrac{1}{10}M'^2)\right\},\end{aligned}\right\} \text{ at } x = x_0. \tag{4.1}$$

These equations imply that

$$\left.\begin{aligned} u' &= Ap' + \text{const.},\\ y\,\partial v'/\partial y &= B\,\partial p'/\partial y,\end{aligned}\right\} \text{ at } x = x_0, \tag{4.2}$$

where
$$A = \frac{M^2+1}{2M^2}\left(\frac{7M^2-1}{M^2+5}\right)^{\frac{1}{2}}, \quad B = \frac{3(M^2-1)}{M^2+5}.$$

Finally, from the first two of equations (3.4) and from equations (4.2) we deduce that

$$\frac{\partial p'/\partial x}{\partial p'/\partial y} = \frac{(A+x_0)\,y - Bx_0/y}{y_0^2} \quad \text{at} \quad x = x_0. \tag{4.3}$$

This is a differential condition for p' and may be supplemented by the requirement that

$$\int_0^{y_0} \frac{1}{y}\frac{\partial p'}{\partial y}\,dy = \frac{1}{B}\int_0^{y_0} \frac{\partial v'}{\partial y}\,dy = \frac{1}{B}\left(v_4' - M_1 - \frac{c_0}{c_1}M'\right). \tag{4.4}$$

The results (4.1) may be used on the portion BI of the shock front by setting $f(y) = (y_3 - y)\,\delta/\epsilon$. This gives

$$\left.\begin{aligned} u_4' &= \tfrac{5}{6}y_3\left\{\left(1+\frac{1}{M^2}\right)\delta/\epsilon + \frac{5M' - M'M^2 - 2M'^2M}{5M^2(M+M')}\right\},\\ v_4' &= M_1\,\delta/\epsilon + (c_0/c_1)\,M',\\ p_3' = p_4' &= \frac{5}{3}\frac{\rho_0}{\rho_1}\frac{c_0}{c_1}y_3\left\{M\delta/\epsilon + \frac{10MM' + 5M^2M'^2 - M'^2}{10(M+M')}\right\}.\end{aligned}\right\} \tag{4.5}$$

In the case of the weak shock ID, the shock equations (2.1) reduce to

$$u_3' = x_2 p_3', \quad v_3' = y_2 p_3', \tag{4.6}$$

and the condition for no flow across the contact discontinuity between regions (3) and (4) is that

$$y_3 u_3' - x_0 v_3' = y_3 u_4' - x_0 v_4'. \tag{4.7}$$

Conditions in regions (3) and (4) are completely determined by the linear equations (4.5), (4.6) and (4.7). In particular p_3' is determined, and we may also find the ratio δ/ϵ of shock deflexion to wedge angle.

Along EA the flow must be parallel to the wedge face. This requires

$$v' = M_1 + (c_0/c_1)\,M'$$

when $y = 0$ so that, using the third of equations (3.4), we get

$$\partial p'/\partial y = 0 \quad \text{when} \quad y = 0. \tag{4.8}$$

5. The boundary-value problem in the Busemann plane

So far no account has been taken of the contact discontinuity in the non-uniform region. Let (r, θ) be polar co-ordinates in the (x, y)-plane of figure 4 so that the approximate position of the contact discontinuity is

$$\theta = \tan^{-1}(y_3/x_0) = \theta^*,$$

say. The second and third of equations (3.4) may now be written as

$$r\,\partial u'/\partial r = \partial p'/\partial x, \quad r\,\partial v'/\partial r = \partial p'/\partial y, \tag{5.1}$$

and the transverse velocity component v_θ' ($= v'\cos\theta - u'\sin\theta$) is seen to satisfy the equation

$$\partial v_\theta'/\partial r = (1/r^2)\,\partial p'/\partial\theta. \tag{5.2}$$

In terms of p', the conditions that pressure and normal flow velocity be continuous across the contact discontinuity would be that p' and $\partial p'/\partial\theta$ are continuous at $\theta = \theta^*$. For $0 \leqslant \theta \leqslant \theta^*$, $0 \leqslant r \leqslant 1$ and for $\theta^* \leqslant \theta \leqslant \pi$, $0 \leqslant r \leqslant 1$, p' satisfies the differential equation (3.5) which becomes, in polar co-ordinates,

$$\frac{\partial^2 p'}{\partial r^2} + \frac{1}{r}\frac{\partial p'}{\partial r} + \frac{1}{r^2}\frac{\partial^2 p'}{\partial\theta^2} = \left(r\frac{\partial}{\partial r} + 1\right)\left(r\frac{\partial p'}{\partial r}\right). \tag{5.3}$$

From the continuity of p' across the radius $\theta = \theta^*$ we deduce the continuity of $\partial p'/\partial r$ and $\partial^2 p'/\partial r^2$ across $\theta = \theta^*$. Hence equation (5.3) shows that

$$\lim_{\theta\to\theta^*-} \frac{\partial^2 p'}{\partial \theta^2} = \lim_{\theta\to\theta^*+} \frac{\partial^2 p'}{\partial \theta^2},$$

so that $\partial^2 p'/\partial\theta^2$ is continuous and equation (5.3) is satisfied across $\theta = \theta^*$. In other words the contact discontinuity does not appear as far as the boundary-value problem for p' is concerned.

Busemann (1943) has shown that, inside the unit circle, the transformation $\bar{r} = (1/r)[1-(1-r^2)^{\frac{1}{2}}]$ reduces equation (5.3) to the equation

$$\frac{\partial^2 p'}{\partial \bar{r}^2} + \frac{1}{\bar{r}}\frac{\partial p'}{\partial \bar{r}} + \frac{1}{\bar{r}^2}\frac{\partial^2 p'}{\partial \theta^2} = 0, \tag{5.4}$$

which is Laplace's equation in polar co-ordinates $\bar{r}$, θ.

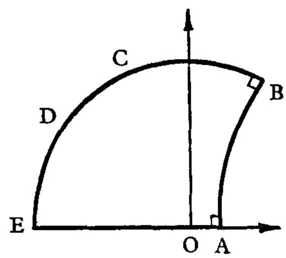

FIGURE 5. The non-uniform region in the $(\bar{r}, \theta)$-plane.

Figure 5 shows the non-uniform region in the $(\bar{r}, \theta)$-plane. The arc BCDE of the unit circle is unchanged and the Cartesian co-ordinates of all points thereon are unchanged. The shock front AB becomes an arc of the circle $2\bar{r}\cos\theta = x_0(1+\bar{r}^2)$ on which, by (4.3) (see Lighthill 1949),

$$\frac{\partial p'/\partial n}{\partial p'/\partial s} = \frac{Ax_0 \tan\theta - B\cot\theta}{(1-x_0^2\sec^2\theta)^{\frac{1}{2}}}, \tag{5.5}$$

$\partial/\partial n$, $\partial/\partial s$ being differentiations normal and tangential to the arc respectively. Condition (4.8) may be written as

$$\partial p'/\partial\theta = 0 \quad \text{when} \quad \theta = \pi, \tag{5.6}$$

in which form it is unchanged by the transformation.

6. Solution by complex-variable method

Write $z = \bar{r}\, e^{i\theta}$, $z_0 = x_0 + iy_0$. We define a new complex variable $\zeta (= \xi + i\eta)$ by the equations

$$\left.\begin{aligned} Z &= z_0\{i - 2y_0/(z-z_0)\}, \\ \zeta = \tfrac{1}{2}(Z^2 + Z^{-2}), &\quad Z^2 = \zeta + (\zeta^2-1)^{\frac{1}{2}}. \end{aligned}\right\} \tag{6.1}$$

Figure 5 represents the complex z-plane and under the conformal mapping (6.1) the boundary ABCDEA of the non-uniform region becomes the entire real axis $\eta = 0$ in the ζ-plane.

We now introduce a function $\omega(\zeta)$ defined by

$$\omega(\zeta) = \partial p'/\partial\eta + i\,\partial p'/\partial\xi,$$

so that, by (5.4), $\omega(\zeta)$ is analytic throughout the upper half-plane. Since

$$\int \omega(\zeta)\,d\zeta = \int\left(\frac{\partial p'}{\partial\eta} + i\frac{\partial p'}{\partial\xi}\right)(d\xi + i\,d\eta),$$

we have

$$p' = \operatorname{Im}\left\{\int \omega(\zeta)\,d\zeta\right\} + \text{const.} \tag{6.2}$$

The circular arc BCDE becomes the portion $\xi < -1$ of the real axis, with C, D corresponding respectively to the points $(\xi_1, 0)$, $(\xi_2, 0)$ where

$$\xi_i = -\frac{(1-x_0x_i)^2 + y_0^2y_i^2}{(1-x_0x_i)^2 - y_0^2y_i^2} \quad (i = 1, 2).$$

The conditions on the circular arc thus become equivalent to the condition that $\omega(\zeta)$ is real for $\eta = 0$, $\xi < -1$ together with

$$\omega(\zeta) \sim -\frac{p_5'}{\pi}\frac{1}{\zeta - \xi_1} \quad \text{at} \quad \zeta = \xi_1, \tag{6.3}$$

$$\omega(\zeta) \sim \frac{p_3'}{\pi}\frac{1}{\zeta - \xi_2} \quad \text{at} \quad \zeta = \xi_2. \tag{6.4}$$

The wedge face EA corresponds to the portion of the real axis where $-1 < \xi < 1$. Here we require that $\omega(\zeta)$ be imaginary.

The shock front AB corresponds to the portion $\xi > 1$ of the real axis, and by (5.5) (see Lighthill 1949) we have here

$$\arg\omega(\zeta) = \tan^{-1}\frac{(\xi-1)^{\frac{1}{2}}}{\gamma_1} + \tan^{-1}\frac{(\xi-1)^{\frac{1}{2}}}{\gamma_2},$$

where

$$\gamma_1, \gamma_2 = \sqrt{2}\,Mx_0\left\{M \pm \frac{M^2-1}{(M^2+5)^{\frac{1}{2}}}\right\}.$$

The required function is given by

$$\omega(\zeta) = \frac{K_1(\zeta-\xi_1) + K_2(\zeta-\xi_2) + K_3(\zeta-\xi_1)(\zeta-\xi_2)}{[\gamma_1 - i(\zeta-1)^{\frac{1}{2}}][\gamma_2 - i(\zeta-1)^{\frac{1}{2}}](\zeta^2-1)^{\frac{1}{2}}(\zeta-\xi_1)(\zeta-\xi_2)} \tag{6.5}$$

with suitable constants K_1, K_2, K_3. Taking $(\zeta^2-1)^{\frac{1}{2}}$ to mean the branch which is positive on the real axis for $\xi > 1$, the conditions (6.3) and (6.4) give

$$K_2 = \pi^{-1}p_5'[\gamma_1 + (1-\xi_1)^{\frac{1}{2}}][\gamma_2 + (1-\xi_1)^{\frac{1}{2}}](\xi_1^2-1)^{\frac{1}{2}},$$
$$K_1 = -\pi^{-1}p_3'[\gamma_1 + (1-\xi_2)^{\frac{1}{2}}][\gamma_2 + (1-\xi_2)^{\frac{1}{2}}](\xi_2^2-1)^{\frac{1}{2}}.$$

From equations (6.1) we find that, corresponding to the shock front, i.e. $\eta = 0$, $\xi > 1$, we have

$$y = y_0\left(\frac{\xi-1}{\xi+1}\right)^{\frac{1}{2}}. \tag{6.6}$$

Hence equation (4.4) gives

$$\begin{aligned}
v_4' - M_1 - \frac{c_0}{c_1} M' &= B\int_1^\infty \frac{1}{y}\frac{\partial p'}{\partial \xi}\,d\xi \\
&= \frac{B}{y_0}\int_1^\infty \left(\frac{\xi+1}{\xi-1}\right)^{\frac{1}{2}} \frac{[K_1(\xi-\xi_1)+K_2(\xi-\xi_2)+K_3(\xi-\xi_1)(\xi-\xi_2)](\gamma_1+\gamma_2)(\xi-1)^{\frac{1}{2}}}{(\gamma_1^2+\xi-1)(\gamma_2^2+\xi-1)(\xi-\xi_1)(\xi-\xi_2)(\xi^2-1)^{\frac{1}{2}}}\,d\xi \\
&= \frac{(\gamma_1+\gamma_2)B}{y_0}\int_0^\infty \frac{K_1(x+\gamma_3^2)+K_2(x+\gamma_4^2)+K_3(x+\gamma_3^2)(x+\gamma_4^2)}{x^{\frac{1}{2}}(x+\gamma_1^2)(x+\gamma_2^2)(x+\gamma_3^2)(x+\gamma_4^2)}\,dx \\
&\qquad \text{where } \gamma_3^2 = 1-\xi_1 > 0,\ \gamma_4^2 = 1-\xi_2 > 0, \\
&= \frac{\pi B}{y_0}\left\{\frac{K_1(\gamma_1+\gamma_2+\gamma_4)}{\gamma_1\gamma_2\gamma_4(\gamma_2+\gamma_4)(\gamma_4+\gamma_1)} + \frac{K_2(\gamma_1+\gamma_2+\gamma_3)}{\gamma_1\gamma_2\gamma_3(\gamma_2+\gamma_3)(\gamma_3+\gamma_1)} + \frac{K_3}{\gamma_1\gamma_2}\right\},
\end{aligned}$$

by the substitution $x = t^2$ and elementary integration. The constant K_3 is thus determined and equation (6.5) gives $\omega(\zeta)$ uniquely.

It can be shown by ordinary integration methods that

$$\int \omega(\zeta)\,d\zeta = -iW(\zeta),$$

where

$$\begin{aligned}
W(\zeta) = {} & C_1\tan^{-1}\left(\frac{\gamma_1-\sqrt{2}}{\gamma_1+\sqrt{2}}\right)^{\frac{1}{2}}\tau + C_2\tan^{-1}\left(\frac{\gamma_2-\sqrt{2}}{\gamma_2+\sqrt{2}}\right)^{\frac{1}{2}}\tau + C_3\tan^{-1}\left(\frac{\gamma_3-\sqrt{2}}{\gamma_3+\sqrt{2}}\right)^{\frac{1}{2}}\tau \\
& + C_4\tan^{-1}\left(\frac{\gamma_4-\sqrt{2}}{\gamma_4+\sqrt{2}}\right)^{\frac{1}{2}}\tau + C_5\tan^{-1}\left(\frac{\gamma_3+\sqrt{2}}{\gamma_3-\sqrt{2}}\right)^{\frac{1}{2}}\tau + C_6\tan^{-1}\left(\frac{\gamma_4+\sqrt{2}}{\gamma_4-\sqrt{2}}\right)^{\frac{1}{2}}\tau,
\end{aligned}$$

$$\tau = \left\{1-\left(\frac{1-\zeta}{2}\right)^{\frac{1}{2}}\right\}\Big/\left(\frac{1+\zeta}{2}\right)^{\frac{1}{2}},$$

and

$$\begin{aligned}
C_1 &= \frac{4}{(\gamma_2-\gamma_1)(\gamma_1^2-2)^{\frac{1}{2}}}\left(\frac{K_1}{\gamma_4^2-\gamma_1^2}+\frac{K_2}{\gamma_3^2-\gamma_1^2}+K_3\right), \\
C_2 &= \frac{4}{(\gamma_1-\gamma_2)(\gamma_2^2-2)^{\frac{1}{2}}}\left(\frac{K_1}{\gamma_4^2-\gamma_2^2}+\frac{K_2}{\gamma_3^2-\gamma_2^2}+K_3\right), \\
C_3 &= \frac{(\gamma_1+\gamma_3)(\gamma_2+\gamma_3)}{(\gamma_1-\gamma_3)(\gamma_2-\gamma_3)}C_5, \quad C_4 = \frac{(\gamma_1+\gamma_4)(\gamma_2+\gamma_4)}{(\gamma_1-\gamma_4)(\gamma_2-\gamma_4)}C_6, \\
C_5 &= \frac{2}{\pi}p_5', \quad C_6 = -\frac{2}{\pi}p_3'.
\end{aligned}$$

It is found that $W(\zeta)$ is purely real when $\eta = 0$, $-1 < \xi < 1$, and that $W(\xi) \to 0$ as $\xi \to -1$. It follows from equation (6.2) that

$$p' = p_5' - \operatorname{Re} W(\zeta)$$

and the solution is now complete.

The behaviour of p' on the wedge face is of special importance. Here the result simplifies to

$$p' = p_5' - W(\xi) \quad (-1 < \xi < 1)$$

and the substitution $\xi = 1-2\{(x_0-x)/(1-x_0x)\}^2$ gives p' in terms of the 'conical' co-ordinate x.

Points immediately behind the shock front correspond to $\eta = 0$, $\xi > 1$. Here we may write

$$\tau = \left(\frac{2}{1+\xi}\right)^{\frac{1}{2}} - i\left(\frac{\xi-1}{\xi+1}\right)^{\frac{1}{2}}$$

and show that

$$\begin{aligned} p' = p_5' - \tfrac{1}{2}\pi(C_5+C_6) \\ -\frac{1}{2}\Bigg\{C_1\tan^{-1}\left(\frac{\gamma_1^2-2}{\xi+1}\right)^{\frac{1}{2}} + C_2\tan^{-1}\left(\frac{\gamma_2^2-2}{\xi+1}\right)^{\frac{1}{2}} + (C_3-C_5)\tan^{-1}\left(\frac{\gamma_3^2-2}{\xi+1}\right)^{\frac{1}{2}} \\ + (C_4-C_6)\tan^{-1}\left(\frac{\gamma_4^2-2}{\xi+1}\right)^{\frac{1}{2}}\Bigg\}, \end{aligned}$$

while $\xi = (y_0^2+y^2)/(y_0^2-y^2)$. This last result enables us to determine the shock position. Writing $F(y) = f(y) - yf'(y)$ we know $F(y)$ in terms of p' from the last of equations (4.1), and the relation

$$f(y) = -y\int y^{-2}F(y)\,dy \tag{6.7}$$

enables us to evaluate $f(y)$ since $f(y_0)$ is known.

7. The nature of the contact discontinuity

Once p' is known, equation (5.1) may be used to find u' and v' by evaluation of integrals along radial lines in the (x, y)-plane, starting from the known values at the boundary. For points at the contact discontinuity $\theta = \theta^*$, the boundary value is chosen in region (3) or region (4) depending on which side the point lies. Thus a genuine discontinuity in u', v' exists at $\theta = \theta^*$ but the discontinuity is of constant amount all along the line. The last of equations (3.4), which can be written as $\partial\rho'/\partial r = \partial p'/\partial r$, shows that a similar discontinuity exists in ρ'.

8. Shock intersection inside sonic circle

Figure 6 is the revised form of figure 4 when $y_3 < y_0$. Regions (3) and (4) have now disappeared; below B the shock is curved and has discontinuous slope at the

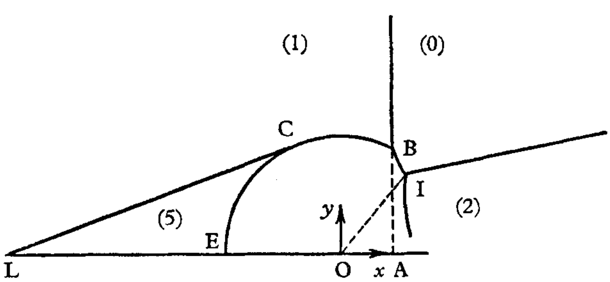

FIGURE 6. Disturbed region in (x, y)-plane when I is inside the sonic circle.

point I which is now regarded as the point of intersection of three shocks and a contact discontinuity. We suppose the tangents to the shock at I make angles δ_1 (upper portion) and δ_2 (lower portion) with the y-axis.

Equations (4.1), omitting terms containing M' and setting

$$f(y) = f(y_3) + (y_3 - y)\,\delta_1/\epsilon,$$

are used to find the limiting values of u', v', p' as we approach I along the upper portion of the shock. To find the limiting values of u', v', p' as we approach I along the lower portion of the shock we use equations (4.1) with

$$f(y) = f(y_3) + (y_3 - y)\,\delta_2/\epsilon.$$

The limiting values of p' must agree while those of u' and v' must satisfy the relation (4.7). Thus the jump $\delta v'$ (say) in v' at I as we cross the contact discontinuity from the lower to the upper portion of the shock can be calculated in terms of $f(y_3)$. Allowance must be made for this discontinuity in v' by subtracting $B^{-1}\delta v'$ from the right-hand side of equation (4.4); we have in addition $v_4' = 0$ and $p_3' = 0$. Finally, since $f(y_3)$ is unknown, we must proceed to equation (6.7) before the solution is complete even for p'.

9. The yawed wedge

The description of the problem in § 2 may be altered in some details for the case of a thin wedge at yaw meeting a plane shock-wave. Figure 7 shows the (X, Z)-plane, in which the leading edge of the wedge is moving with supersonic

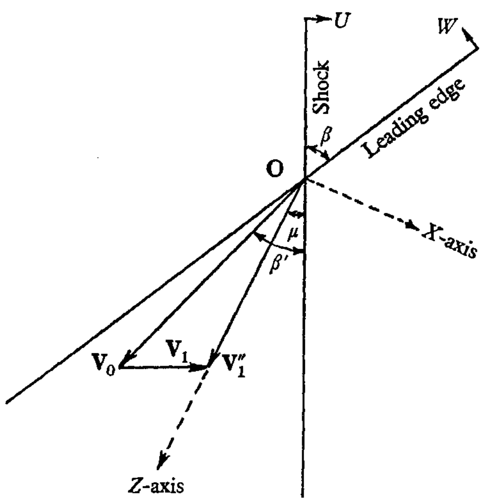

FIGURE 7. The (X, Z)-plane.

velocity W, and we again assume the plane of symmetry of the wedge to lie approximately in this plane. The shock front has velocity U and makes an angle β with the leading edge. The point O where the leading edge intersects the shock front may be brought to rest by superimposing on the entire system a velocity $\mathbf{V}_0$ whose magnitude V_0 is $\operatorname{cosec}\beta(U^2 + W^2 + 2UW\cos\beta)^{\frac{1}{2}}$ and whose direction makes an angle $\beta' = \sin^{-1}(U/V_0)$ with the shock front; the flow is then steady, and the three-dimensional nature of the problem is offset by the suppression of the time variable.

The uniform flow behind the shock now has velocity $\mathbf{V}_1'' = \mathbf{V}_1 + \mathbf{V}_0$; the direction of $\mathbf{V}_1''$ makes an angle μ with the shock front where

$$\tan\mu = (U - V_1)\sin\beta/(W + U\cos\beta)$$

and its magnitude is given by

$$V_1''^2 = (U - V_1)^2 + \{(W + U\cos\beta)/\sin\beta\}^2.$$

It can be shown that $V_1'' > c_1$ if $\beta < \beta_1 + \beta_2$ or $\beta > \pi - \beta_1 + \beta_2$, where

$$\beta_1 = \sin^{-1}\left\{\frac{\sqrt{6}\,MM'}{(7M^4 + 4M^2 - 5)^{\frac{1}{2}}}\right\}, \quad \beta_2 = \tan^{-1}\left\{\frac{\sqrt{6}\,M^2}{(M^2-1)^{\frac{1}{2}}\,(M^2+5)^{\frac{1}{2}}}\right\}.$$

This means that for any fixed wedge speed the point (M, β) must lie to the left of the appropriate curve as illustrated in figure 8. (The common asymptote is $\beta = \tan^{-1}\sqrt{6} = 67{\cdot}8°$.)

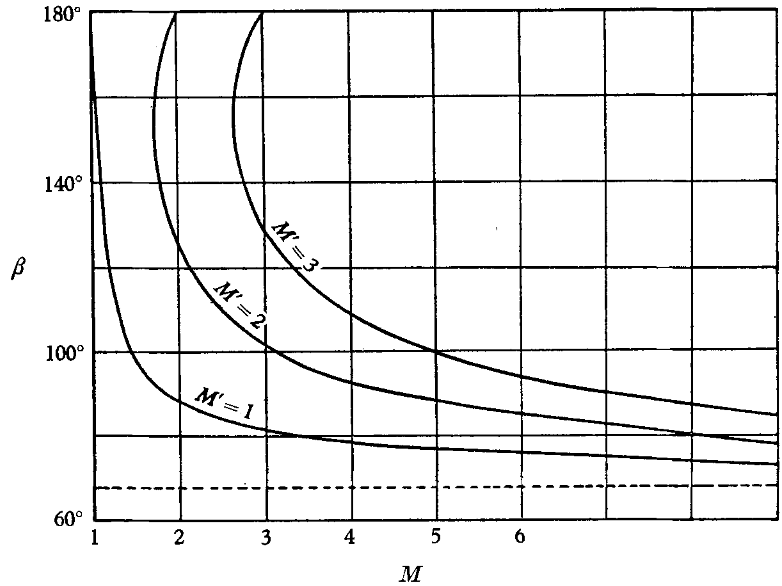

FIGURE 8. The range of β for which the flow behind the shock is supersonic.

The subsequent treatment relies on supersonic flow behind the shock so we shall assume β lies within the required range and furthermore that $\beta < \frac{1}{2}\pi$. The point O is taken as origin with the Z-axis in the direction of $\mathbf{V}_1''$, and the Mach cone with semi-angle α, where $\sin\alpha = c_1/V_1'' = c_1\sin\mu/(U - V_1)$, is drawn on this axis with O as vertex. The region of non-uniform flow is bounded below by the wedge face, ahead by the shock-front, and elsewhere by the Mach cone. (We again consider the flow above the wedge only since the flow above and below are independent.) The tangent plane from the leading edge of the wedge to the Mach cone is a weak shock-front; between this and the cone is a uniform region (5) in which the flow is parallel to the wedge face. A similar weak shock front is attached to the portion of the leading edge which lies ahead of the advancing shock; it makes an angle ϕ_0 with the (X, Z)-plane $(\cot\phi_0 = (M'^2 - 1)^{\frac{1}{2}})$ and separates the region (2) of uniform flow parallel to the wedge face from the main region (0) ahead of the shock. Across this shock, equations (2.1) give

$$\rho_2 = \rho_0[1 + \epsilon M'^2/(M'^2 - 1)^{\frac{1}{2}}], \quad p_2 = p_0[1 + \epsilon\, 7M'^2/5(M'^2 - 1)^{\frac{1}{2}}], \quad \mathbf{V}_2 = \mathbf{V}_0 - \epsilon W\mathbf{k},$$

where $\mathbf{k}$ is a unit vector in the direction $[\tan\phi_0, -1, \tan\phi_0\tan(\beta - \mu)]$.

The weak shock between regions (0) and (2) meets the main shock along a line l through the origin. The tangent plane from l on to the Mach cone is another weak shock-front, and the plane containing l and the Z-axis is the approximate position of a contact discontinuity surface; between the weak shock, the Mach cone, and the main shock are two uniform regions (3) and (4) separated by the contact discontinuity.

Within the region of non-uniform flow we use the equations of steady rotational three-dimensional flow, i.e. the equations (3.1) omitting time derivatives. We further assume

$$\left.\begin{aligned} p &= p_1+\epsilon p^{(1)}(X,Y,Z)+\epsilon^2 p^{(2)}(X,Y,Z)+\dots, \\ \rho &= \rho_1+\epsilon \rho^{(1)}(X,Y,Z)+\epsilon^2 \rho^{(2)}(X,Y,Z)+\dots, \\ \mathbf{V} &= \mathbf{V}_1''+\epsilon \mathbf{V}^{(1)}(X,Y,Z)+\epsilon^2 \mathbf{V}^{(2)}(X,Y,Z)+\dots. \end{aligned}\right\} \tag{9.1}$$

The lack of a fundamental length scale in the problem suggests that the flow variables are functions of the two independent variables x, y defined by

$$x = X/Z\tan\alpha, \quad y = Y/Z\tan\alpha.$$

Dimensionless variables may be defined as before; we write

$$p' = p^{(1)}/\rho_1 c_1^2, \quad \rho' = \rho^{(1)}/\rho_1, \quad \mathbf{V}' = (1/c_1)\,\mathbf{V}^{(1)} = \{u'\cos\alpha,\, v'\cos\alpha,\, -w'\sin\alpha\}.$$

From the equations of motion we may now reproduce the equations (3.4) together with the additional equation

$$x\frac{\partial w'}{\partial x}+y\frac{\partial w'}{\partial y} = \frac{\partial u'}{\partial x}+\frac{\partial v'}{\partial y}.$$

Figure 4 may be used to represent the configuration in the (x,y)-plane; the following amendments to the co-ordinates of the important points are all that is necessary:

$$x_0 = \frac{\tan\mu}{\tan\alpha} = \left(\frac{M^2+5}{7M^2-1}\right)^{\frac{1}{2}}\frac{\cos\alpha}{\cos\mu},$$

$$y_3 = \frac{\tan\mu+\tan(\beta-\mu)}{\tan\alpha}\tan\phi_0 = \frac{6M\cos\alpha(M\cos\beta+M')}{\cos^2\mu\cos^2(\beta-\mu)\,[(7M^2-1)(M^2+5)(M'^2-1)]^{\frac{1}{2}}},$$

$$x_1 = -\frac{1}{[\{(c_0/c_1)\,M'+M_1\cos\beta\}^2\cos^2(\beta-\mu)+\sin^2(\beta-\mu)]^{\frac{1}{2}}}.$$

The solution procedure outlined for the case of a normal shock may now be followed exactly; the revised form of the main results used is given below, where all the formulae are expressed in a form which indicates clearly the limit as $\beta\to 0$. We have

$$p_5' = \{(c_0/c_1)\,M'+M_1\cos\beta\}^2/\{[(c_0/c_1)\,M'+M_1\cos\beta]^2-1\}^{\frac{1}{2}}.$$

The equations (4.1) become

$$\begin{aligned} u' &= \frac{5\cos\mu}{6\cos\alpha}\left\{\frac{\cos^2\mu}{\cos\alpha}\frac{(M^2+M'^2+2MM'\cos\beta)^{\frac{1}{2}}}{M'+M\cos\beta}\left[\cos(\beta'+\mu)+\frac{1}{M^2}\cos(\beta'-\mu)\right]\right. \\ &\qquad\left.\times\{f(y)-yf'(y)\}+\frac{c_0/c_1}{(M'^2-1)^{\frac{1}{2}}}\left[\frac{M'\cos\beta}{M^2}-(\tfrac{6}{5}\sec\mu-\cos\beta)\,M'-\frac{2}{5}\frac{M'^2}{M}\right]\right\}, \\ v' &= -M_1 f'(y)\frac{\cos\mu}{\cos\alpha}+\frac{c_0}{c_1}\frac{M'}{\cos\alpha}, \\ p' &= \frac{5}{3}\frac{\rho_0}{\rho_1}\frac{c_0}{c_1}\left\{\frac{\cos^3\mu}{\cos\alpha}M(f(y)-yf'(y))+\frac{c_0/c_1}{(M'^2-1)^{\frac{1}{2}}}(MM'\cos\beta+\tfrac{1}{2}M^2M'^2-\tfrac{1}{10}M'^2)\right\}, \end{aligned}$$

from which, in equations (4.2), we have

$$A = \left(\frac{7M^2-1}{M^2+5}\right)^{\frac{1}{2}} \frac{M^2\cos(\beta'+\mu)+\cos(\beta'-\mu)}{2M^2\cos\alpha\cos\beta'}, \quad B = \frac{3(M^2-1)}{M^2+5}\sec^2\mu.$$

The alterations to equations (4.5) follow immediately from those to equations (4.1). The right-hand side of equation (4.4) is replaced by

$$(1/B)\,[v_4' - \{M_1\cos\beta + (c_0/c_1)\,M'\}\sec\alpha],$$

while equations (4.6) should read

$$u_3'\cos\alpha = x_2 p_3', \quad v_3'\cos\alpha = y_2 p_3'.$$

No alteration in form is necessary to equation (4.7).

10. Numerical results

The pressure distribution on the wedge face has been calculated in a number of cases and the results are illustrated by figures 9, 10 and 11 which demonstrate,

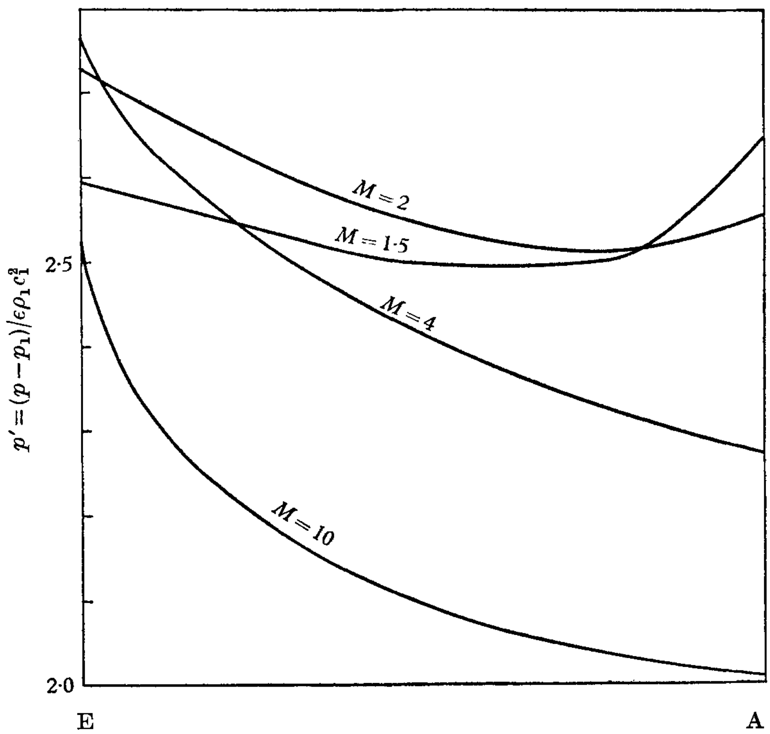

FIGURE 9. The pressure distribution on the portion EA of the wedge face when $\beta = 0$, $M' = 2$ with various values of M.

respectively, the effect of shock strength, wedge speed, and yaw. Only the portion EA of the wedge face, on which pressure is non-constant, is shown and the scale is adjusted to make the distance EA the same in all cases.

11. Aerofoil of arbitrary shape

The methods used so far are limited to infinite wedges. Consider now a multiple wedge with n faces and corresponding directional changes ϵ_i ($i = 1, 2, \ldots, n$), all small (see figure 12).

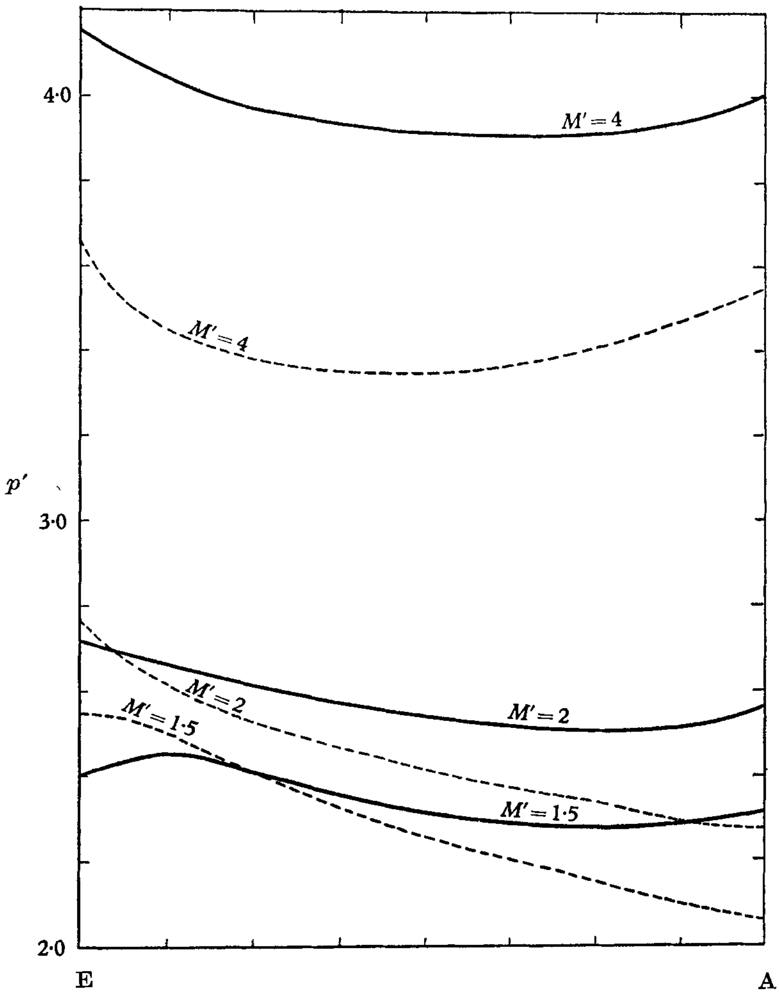

FIGURE 10. The pressure distribution along EA when $\beta = 0$, $M = 2$ with various values of M'. The corresponding results with M increased to 4 are given by the broken curves.

We write, in place of (3.2),

$$p = p_1 + \sum_{i=1}^{n} \epsilon_i p^{(1,i)}(X, Y, t) + \ldots,$$

since ϵ_i are independent parameters. Moreover, setting $\epsilon_i = 0$ $(i \neq j)$ we see that $p^{(1,j)}$ can be identified in terms of the function $p^{(1)}$ associated with the single wedge; using moving axes as in § 2, we have

$$p^{(1,j)} = p^{(1)}\left(X - \frac{s_{j-1}(U - V_1)}{U + W}, Y, t - \frac{s_{j-1}}{U + W}\right).$$

Thus the functions $p^{(1,j)}$ correspond to disturbances differing only in space and time origins. If any of ϵ_i are negative the corresponding single wedge solution is still applicable; in that case the weak attached shocks are interpreted as weak expansion waves.

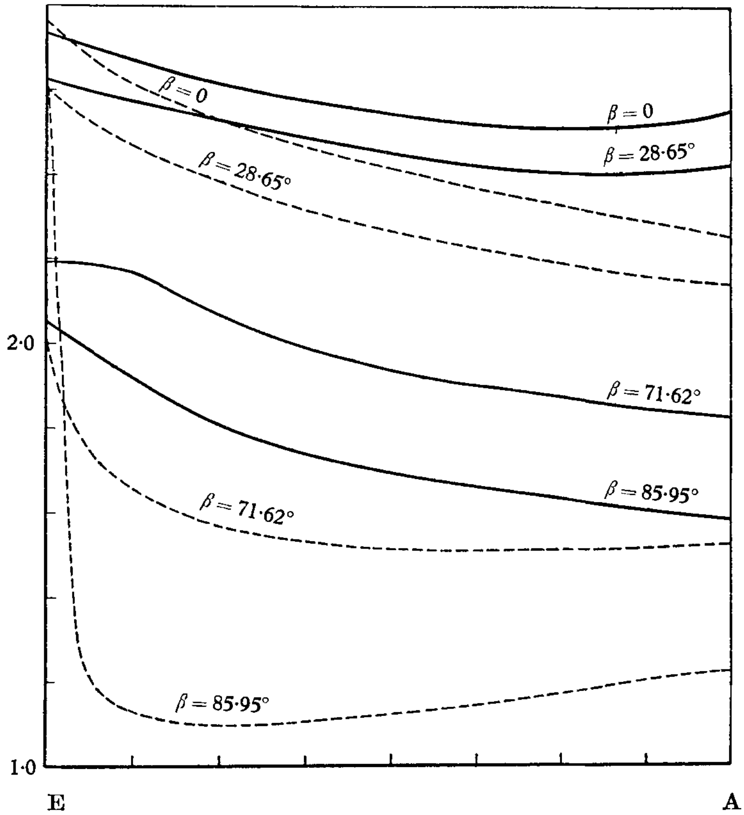

FIGURE 11. The pressure distribution along EA when $M' = 2$, $M = 2$ with $\beta = 0$, 0·5, 1·25, 1·5 radians respectively. The corresponding results with M increased to 4 are given by the broken curves.

For an aerofoil of arbitrary profile, let s denote distance from the leading edge in the direction of the X-axis and let the upper surface of the aerofoil have equation $Y = \psi(s)$ where $\psi(s)$ is uniformly small. By a simple limiting process we find

$$p = p_1 + \int_0^\infty p^{(1)}\left(X - \frac{s(U-V_1)}{U+W}, Y, t - \frac{s}{U+W}\right)\psi''(s)\,ds.$$

The variable region of non-zero $p^{(1)}$ which is encountered in the integrand makes it convenient to express p in another form. Writing

$$x = \left(X - \frac{s(U-V_1)}{U+W}\right)\Big/ c_1\left(t - \frac{s}{U+W}\right), \quad y = Y \Big/ c_1\left(t - \frac{s}{U+W}\right), \qquad (11.1)$$

we know that $p^{(1)}$ is, for all, X, Y, t and s, a function of x and y only; we denote this function by $p^{(1)}(x,y)$. Eliminating s between equations (11.1), we find that the path of integration in the (x,y)-plane is the straight line

$$y_P(x-x_0) + y(x_0 - x_P) = 0, \quad \text{where} \quad x_P = X/c_1 t, \quad y_P = Y/c_1 t.$$

The situation can now be referred to the (x, y)-plane of figure 4 where, to find the pressure at a point P with co-ordinates (x_P, y_P) we evaluate

$$p_1 + \int p^{(1)}(x, y)\, \psi''\left(\frac{(U+W)\,(x_P - x)}{x_0 - x}\, t\right) dl, \tag{11.2}$$

where integration is along the straight line PQ. (PQ passes through A, and Q is the point where it meets the boundary separating the disturbance region from region (1).) For points on the surface of the aerofoil we have straightforward integrations along the x-axis.

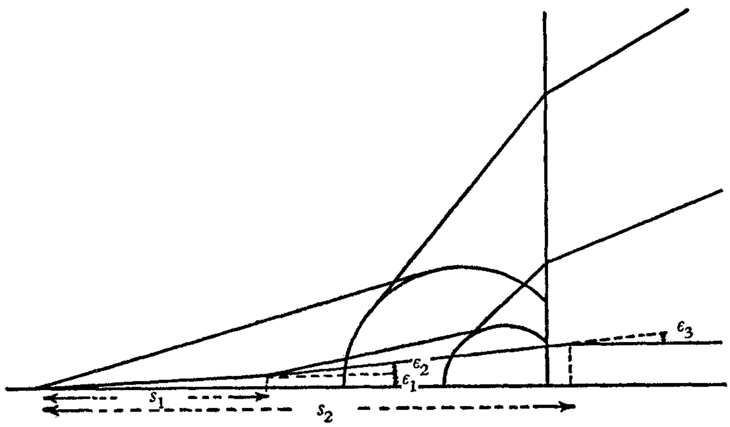

FIGURE 12. Shock-wave meeting multiple wedge.

The solution for an infinite wedge at yaw can similarly be extended. We find

$$p = p_1 + \int p^{(1)}(x, y)\, \psi''\left(\frac{x_P - x}{x_0 - x}\, Z \sin\beta\right) dl, \tag{11.3}$$

where $p^{(1)}$ refers to the wedge at yaw as in § 9, and integration is again along the line PQ in figure 4. Remembering that the axes used in § 9 move differently from those used for the normal shock, we can easily verify that the limit of (11.3) as $\beta \to 0$ is (11.2). In a similar manner the other flow variables and the position of the shock front can be calculated from the wedge solution.

The author wishes to express his gratitude to Prof. D. C. Pack who first introduced him to this problem and whose unfailing interest in the progress of the work was a great source of encouragement. He is also indebted to the referee for suggesting the extension of the work to yawed wedges.

REFERENCES

BUSEMAN, A. 1943 *Luftfahrtforsch.* **20**, 105.

CHESTER, W. 1954 *Quart. J. Mech. Appl. Math.* **7**, 57.

COURANT, R. & FRIEDRICHS, K. O. 1948 *Supersonic Flow and Shock Waves*, ch. 4E, § 141. New York: Interscience.

EHLERS, F. E. & SHOEMAKER, E. M. 1959 *J. Aero/Space Sci.* **26**, 75.

LIGHTHILL, M. J. 1949 *Proc. Roy. Soc.* A, **198**, 454.

LUDLOFF, H. F. & TING, L. 1951 *J. Aero. Sci.* **18**, 143.

LUDLOFF, H. F. & TING, L. 1952 *J. Aero. Sci.* **19**, 317.

VON MISES, R. 1958 *Mathematical Theory of Compressible Fluid Flow*, ch. 5, § 23. New York: Academic Press.

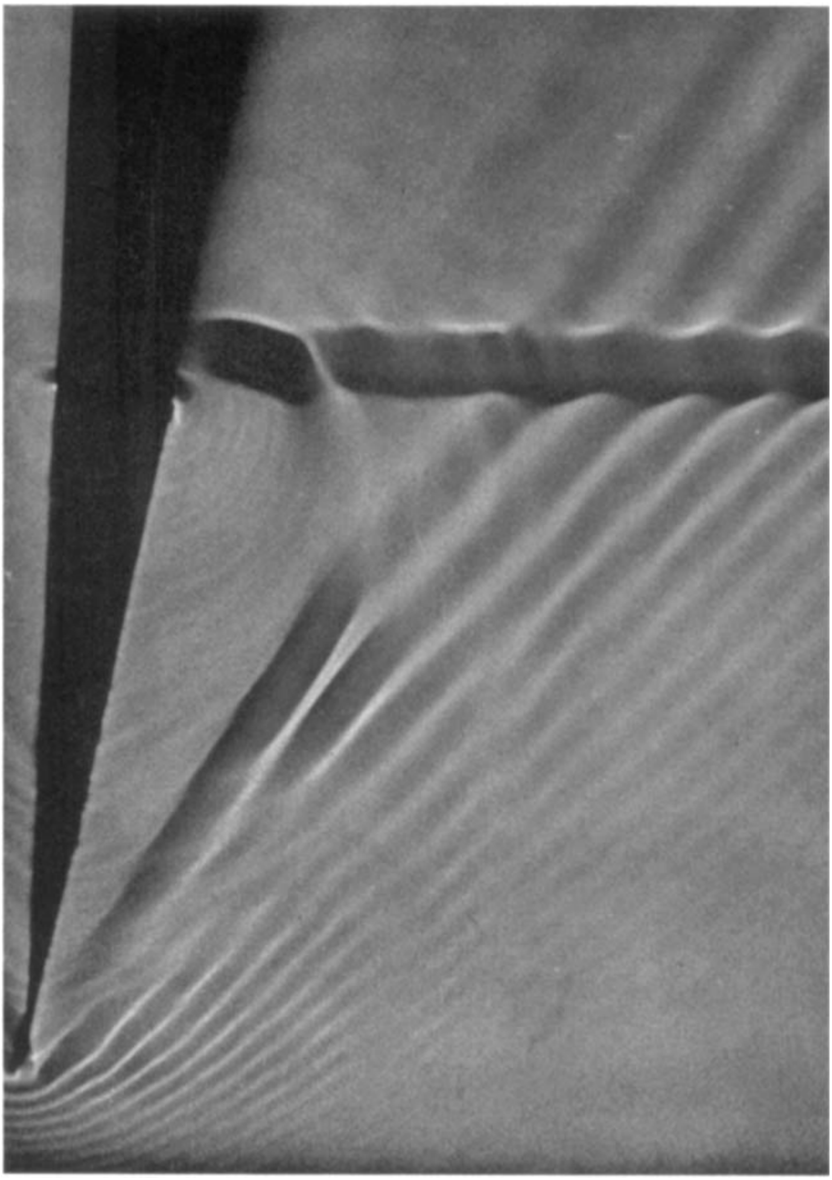

FIGURE 2. Bore meeting wedge in super-critical flow in shallow water tank. Photograph taken by E. J. Klein in the Hydraulics Laboratory, The Royal College of Science and Technology, Glasgow.